3-2015

Optimization-Free Optical Focal Field Engineering through Reversing the Radiation Pattern from a Uniform Line Source

Yanzhong Yu
University of Dayton

Qiwen Zhan
University of Dayton, qzhan1@udayton.edu

Optimization-free optical focal field engineering through reversing the radiation pattern from a uniform line source

Yanzhong Yu[1,2,3] and Qiwen Zhan[2,*]

[1]*College of Physics & Information Engineering, Quanzhou Normal University, Fujian 362000, China*
[2]*Electro-Optics Program, University of Dayton, 300 College Park, Dayton, Ohio 45469, USA*
[3]*yuyanzhong059368@gmail.com*
**qzhan1@udayton.edu*

Abstract: A simple and flexible method is presented for the generation of optical focal field with prescribed characteristics. By reversing the field pattern radiated from a uniform line source, for which the electric current is constant along its extent, situated at the focus of a 4Pi focusing system formed by two confocal high-NA objective lenses, the required illumination distribution at the pupil plane for creating optical focal field with desired properties can be obtained. Numerical example shows that an arbitrary length optical needle with extremely high longitudinal polarization purity and consistent transverse size of ~0.36λ over the entire depth of focus (DOF) can be created with this method. Coaxially double-focus with spot size of ~0.36λ in the transversal direction and ~λ in the axial direction separated by a prescribed spacing is illustrated as another example. The length of optical needle field and the interval between double-focus are determined by the length of uniform line source. These engineered focal fields may found potential applications in particle acceleration, optical microscopy, optical trapping and manipulations.

OCIS codes: (260.5430) Polarization; (050.1970) Diffractive optics; (350.5610) Radiation.

References and links

1. Q. Zhan, "Cylindrical vector beams: from mathematical concepts to applications," Adv. Opt. Photon **1**(1), 1–57 (2009).
2. Q. Zhan and J. R. Leger, "Focus shaping using cylindrical vector beams," Opt. Express **10**(7), 324–331 (2002).
3. T. Kuga, Y. Torii, N. Shiokawa, T. Hirano, Y. Shimizu, and H. Sasada, "Novel optical trap of atoms with a doughnut beam," Phys. Rev. Lett. **78**(25), 4713–4716 (1997).
4. S. Sato, Y. Harada, and Y. Waseda, "Optical trapping of microscopic metal particles," Opt. Lett. **19**(22), 1807–1809 (1994).
5. W. D. Kimura, G. H. Kim, R. D. Romea, L. C. Steinhauer, I. V. Pogorelsky, K. P. Kusche, R. C. Fernow, X. Wang, and Y. Liu, "Laser acceleration of relativistic electrons using the inverse Cherenkov effect," Phys. Rev. Lett. **74**(4), 546–549 (1995).
6. S. Payeur, S. Fourmaux, B. E. Schmidt, J. P. MacLean, C. Tchervenkov, F. Légaré, M. Piché, and J. C. Kieffer, "Generation of a beam of fast electrons by tightly focusing a radially polarized ultrashort laser pulse," Appl. Phys. Lett. **101**(4), 041105 (2012).
7. Y. J. Yoon, W. C. Kim, N. C. Park, K. S. Park, and Y. P. Park, "Feasibility study of the application of radially polarized illumination to solid immersion lens-based near-field optics," Opt. Lett. **34**(13), 1961–1963 (2009).
8. G. Terakado, K. Watanabe, and H. Kano, "Scanning confocal total internal reflection fluorescence microscopy by using radial polarization in the illumination system," Appl. Opt. **48**(6), 1114–1118 (2009).
9. H. Dehez, M. Piché, and Y. De Koninck, "Enhanced resolution in two-photon imaging using a TM01 laser beam at a dielectric interface," Opt. Lett. **34**(23), 3601–3603 (2009).
10. H. Wang, G. Yuan, W. Tan, L. Shi, and T. Chong, "Spot size and depth of focus in optical data storage system," Opt. Eng. **46**(6), 065201 (2007).
11. H. F. Wang, L. P. Shi, B. Lukyanchuk, C. Sheppard, and C. T. Chong, "Creation of a needle of longitudinally polarized light in vacuum using binary optics," Nat. Photonics **2**(8), 501–505 (2008).
12. T. Liu, J. B. Tan, J. Liu, and J. Lin, "Creation of subwavelength light needle, equidistant multi-focus, and uniform light tunnel," J. Mod. Opt. **60**(5), 378–381 (2013).
13. J. Wang, W. Chen, and Q. Zhan, "Three-dimensional focus engineering using dipole array radiation pattern," Opt. Commun. **284**(12), 2668–2671 (2011).

14. Y. Zhao, Q. Zhan, Y. Zhang, and Y. P. Li, "Creation of a three-dimensional optical chain for controllable particle delivery," Opt. Lett. **30**(8), 848–850 (2005).
15. K. Huang, P. Shi, X. L. Kang, X. B. Zhang, and Y. P. Li, "Design of DOE for generating a needle of a strong longitudinally polarized field," Opt. Lett. **35**(7), 965–967 (2010).
16. N. Bokor and N. Davidson, "Toward a spherical spot distribution with 4pi focusing of radially polarized light," Opt. Lett. **29**(17), 1968–1970 (2004).
17. Z. Chen, J. Pu, and D. Zhao, "Generating and shifting a spherical focal spot in a 4Pi focusing system illuminated by azimuthally polarized beams," Phys. Lett. A **377**(34–36), 2231–2234 (2013).
18. Z. Chen and D. Zhao, "4Pi focusing of spatially modulated radially polarized vortex beams," Opt. Lett. **37**(8), 1286–1288 (2012).
19. S. Yan, B. Yao, and R. Rupp, "Shifting the spherical focus of a 4Pi focusing system," Opt. Express **19**(2), 673–678 (2011).
20. T. Liu, J. Tan, J. Lin, and J. Liu, "Generating super-Gaussian light needle of 0.36λ beam size and pure longitudinal polarization," Opt. Eng. **52**(7), 074104 (2013).
21. J. Liu, M. Ai, J. Tan, R. Wang, and X. Tan, "Focusing of cylindrical-vector beams in elliptical mirror based system with high numerical aperture," Opt. Commun. **305**, 71–75 (2013).
22. W. Chen and Q. Zhan, "Creating a spherical focal spot with spatially modulated radial polarization in 4Pi microscopy," Opt. Lett. **34**(16), 2444–2446 (2009).
23. J. Wang, W. Chen, and Q. Zhan, "Engineering of high purity ultra-long optical needle field through reversing the electric dipole array radiation," Opt. Express **18**(21), 21965–21972 (2010).
24. W. Chen and Q. Zhan, "Diffraction limited focusing with controllable arbitrary three-dimensional polarization," J. Opt. **12**(4), 045707 (2010).
25. J. Wang, W. Chen, and Q. Zhan, "Three-dimensional focus engineering using dipole array radiation pattern," Opt. Commun. **284**(12), 2668–2671 (2011).
26. W. L. Stutzman and G. A. Thiele, *Antenna Theory and Design*, 2nd Edition (J. Wiley, 1998).
27. E. Wolf, "Electromagnetic diffraction in optical systems I. An integral representation of the image field," Proc. R. Soc. Ser. A **253**, pp. 349–357 (1959).
28. B. Richards and E. Wolf, "Electromagnetic diffraction in optical system II. Structure of the image field in an aplanatic system," Proc. R. Soc. Ser. A **253**, pp. 358–379 (1959).
29. K. S. Youngworth and T. G. Brown, "Focusing of high numerical aperture cylindrical-vector beams," Opt. Express **7**(2), 77–87 (2000).
30. H. Dehez, A. April, and M. Piché, "Needles of longitudinally polarized light: guidelines for minimum spot size and tunable axial extent," Opt. Express **20**(14), 14891–14905 (2012).
31. R. Liu, B. Z. Dong, G. Z. Yang, and B. Y. Gu, "Generation of pseudo-nondiffracting beams with use of diffractive phase elements designed by the conjugate-gradient method," J. Opt. Soc. Am. A **15**(1), 144–151 (1998).
32. W. Han, Y. Yang, W. Cheng, and Q. Zhan, "Vectorial optical field generator for the creation of arbitrarily complex fields," Opt. Express **21**(18), 20692–20706 (2013).

1. Introduction

In recent years, three-dimensional (3D) focus engineering with cylindrical vector (CV) beams [1, 2] has received increasing interests due to its novel properties and potential applications in many areas such as optical trapping and manipulation [3, 4], particle acceleration [5, 6], microscopy [7–9], and high-density optical data storage [10]. A large number of methods for creating specific focusing patterns, such as optical needle [11], optical tunnel [12, 13], and optical chain [14], have been reported both theoretically and experimentally. These methods can be roughly classified into four categories. Firstly, an approach by tight focusing a radially polarized Bessel-Gaussian (BG) beam with a high numerical aperture (NA) objective lens and a diffractive optical element (DOE) was suggested to generate a longitudinally polarized light needle with small radial beam size and ultra-long depth of focus (DOF) [11, 15]. Secondly, a scheme to create a spherical focal spot in the focus region was proposed by focusing radially or azimuthally polarized beams in a 4Pi focusing system [16–19]. Thirdly, modulating the radially polarized beam by specific filter under a reflection mirror system was established to produce super-Gaussian light needle [20, 21]. Lastly, a novel method for 3D focus engineering was developed more recently through reversing the electric field radiated from a dipole antenna or a dipole array [22–25].

In the present work, a simple and more flexible approach that falls into the last category is demonstrated to create optical focal fields with desired properties. Instead of a dipole array [23, 25], this method utilizes the reversing of the radiation field of a uniform line source for which the electric current is constant along its extent [26]. As examples, a high purity optical needle field with arbitrarily chosen length and a coaxial double-focus with desired spacing are

#232538 - $15.00 USD Received 15 Jan 2015; revised 2 Mar 2015; accepted 4 Mar 2015; published 13 Mar 2015

created using this method. Compared with the method described in articles [23, 25] that requires the optimization of 3N parameters related to a dipole array with 2N elements, the current method does not require any optimization procedure, significantly simplifying the design procedure. In addition, the transverse size of the optical needle realized with this method is 10% (0.36λ vs. 0.405λ) smaller than that reported with the previous method using dipole array.

2. Method

The excellent focusing capability of a radially polarized beam can be regarded as the time-reversed propagation of the radiation field from an electric dipole collected by an objective lens at the pupil plane [1]. This explanation was exploited and developed to generate a high purity ultra-long optical needle field by backward propagating radiation field of an electric dipole array with 2N dipole elements [23]. However the DOF of an optical needle field engineered in [23] is mainly determined by the total number of elements of dipole array and the number of parameters needed to be optimized increases as 3N for a 2N-element dipole array. Obviously, as N increases, the optimization difficulty increases as well. To overcome these disadvantages, in the present paper the radiation field of a uniform line source is used in place of that of a dipole array. The idea for the proposed method stems from the explanation that the ultra-long optical needle with high-purity longitudinal polarization and small transverse spot can be considered as a uniform line source on which electric current is directed at the z-direction and constant along its extent (see Fig. 1). Therefore, in order to obtain this optical needle field, one can reverse and focus the entire optical field radiated from the uniform line source. Because of the spherical wavefront of this radiation field, a 4Pi focusing system [16–19] is employed to gather and reversely propagate the entire propagating radiation field back to the focus volume. The schematic for the proposed method is shown in Fig. 1. A uniform line source situated at the focus of the 4Pi focusing system consisting of two confocal high-NA objectives is aligned along the optical axis. The current distribution for the uniform line source centered on the focus and along the z-axis can be written as [26]

$$I(z') = \begin{cases} I_0 & x' = 0,\ y'=0,\ |z'| \le L/2 \\ 0 & elsewhere \end{cases} \tag{1}$$

where I_0 denotes the constant current and L is the length of the line source. The electric field radiated by uniform line source on the spherical surface with radius f is given by [26]

$$\vec{F}(\theta) = C \sin\theta \frac{\sin[(kL/2)\cos\theta]}{(kL/2)\cos\theta} \vec{e}_\theta \tag{2}$$

where $C = j\omega\mu I_0 L \exp(-jkf)/4\pi f$, ω and μ denote the angular frequency and the permeability, respectively, k and f represent respectively the wave numbers and the focal length of the 4Pi focusing system, θ is the angle between radiation direction and optical axis, and $\vec{e}_\theta$ is unit vector of the radiation field. For the convenience of computing, C is normalized to 1 in our work. By combining the radiation field given in Eq. (2) with the Richards–Wolf vectorial diffraction theory [27, 28], the required incident field at the pupil plane of high-NA objective lens for generating the desired focal field can be derived analytically through solving the inverse problem. For an aplanatic objective lens that obeys the sine condition, the required input field $\vec{E}_i(r)$ at the pupil plane can be expressed by

$$\vec{E}_i(r) = \vec{F}(\theta)\big/\sqrt{\cos\theta} \tag{3}$$

where $r = f\sin\theta$. If the incident field distribution $\vec{E}_i(r)$ is used as illumination at the pupil plane and reversely propagates to the focal volume of 4Pi focusing system, as indicated by the

#232538 - $15.00 USD Received 15 Jan 2015; revised 2 Mar 2015; accepted 4 Mar 2015; published 13 Mar 2015

red arrows (see Fig. 1), the focus field can be evaluated by the Richards–Wolf vectorial diffraction integral as [27–29]

$$E_r(r,z) = 2A\int_0^{\theta_{\max}} E_i(r)P(\theta)\sin\theta\cos\theta J_1(kr\sin\theta)\exp(ikz\cos\theta)d\theta \tag{4}$$

$$E_z(r,z) = j2A\int_0^{\theta_{\max}} E_i(r)P(\theta)\sin^2\theta J_0(kr\sin\theta)\exp(ikz\cos\theta)d\theta \tag{5}$$

Here $E_r(r,z)$ and $E_z(r,z)$ are the radial and longitudinal field components at the observation point (r,z), respectively. A is the amplitude constant and $P(\theta)=\sqrt{\cos(\theta)}$ is the pupil apodization function of aplanatic lens. $\theta_{\max}$ is the maximal focusing angle determined by the NA of the objective lens. J_m denotes the mth -order Bessel function of the first kind.

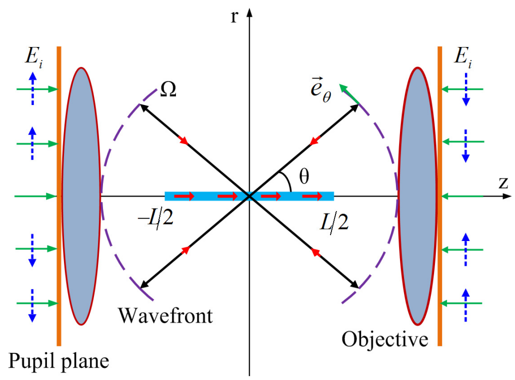

Fig. 1. Schematic of the proposed method. The uniform line source centered on the focus of 4Pi focusing system consisting of two confocal high-NA objective lenses is aligned along the optical axis. The radiation field is entirely collected and reversely propagated to the focus volume.

3. Numerical examples

3.1 Generation of high purity optical needle field with desired length

In order to entirely gather the radiation field, the maximum focusing angle $\theta_{\max}$ of the 4Pi focusing system is chosen to be $\theta_{\max} = \pi/2$. This corresponds to $NA = 1.0$ in free space. Assuming that the 4Pi focusing system is illuminated by two counter-propagating radially polarized beams $\vec{E}_i(r)$ with a relative π phase shift, one can obtain the optical needle field distribution in the vicinity of focus volume. The total electric energy densities, $|E|^2 = |E_r|^2 + |E_z|^2$, in r-z plane, corresponding phase distributions of the E_z component, and axial electric energy densities, $|E(0,z)|^2$, for $L = 4\lambda, 6\lambda, 8\lambda, 10\lambda$ are illustrated in Figs. 2(a)-2(c), respectively to demonstrate the simplicity and flexibility of the proposed method. A FWHM radial spot size of 0.36λ (i.e. spot area $\sim 0.10\lambda^2$) that may have approached the minimum size in free space [20, 30] is achieved and independent of parameter L, which is smaller than that obtained by using electric dipole array radiation (FWHM = 0.405λ) [23]. Therefore, the spot area is reduced by 21%. Moreover, the FWHM remains $\sim 0.36\lambda$ within the entire length of the optical needle field. From Fig. 2(b), one also can see that the phase of the E_z component for the main lobe remains constant at -90° along the entire DOF with a length equal to the length of uniform line source L. The phase distribution within the focal region is a very crucial factor for the creation of a high quality optical needle field that has not received attention previously. It is important to keep the phase constant. Otherwise the phase fluctuation would cause the instantaneous electric field to fluctuate along the optical axis, deteriorating the quality of the created optical needle field. It can be observed from Fig. 2(c) that the depth of focus (DOF, defined as the axial full width of above 80% maximum intensity) is close to the length of uniform line source and is mainly determined by parameter L.

To evaluate the uniformity of axial energy density distribution over a DOF region, we introduce a nonuniformity γ defined in the form of $\gamma = \sqrt{(\langle I^2 \rangle - \langle I \rangle^2)} \big/ \langle I \rangle$ [31], where $I = |E(0,z)|^2$ and $\langle ... \rangle$ denotes the average value of the related quantity over a given range. Then we can obtain $\gamma = 3.36\%, 2.75\%, 2.24\%, 2.01\%$ within the entire DOF, corresponding to $L = 4\lambda, 6\lambda, 8\lambda, 10\lambda$, respectively. This indicates that the uniformity of axial energy density distribution improves with increasing length L. We further calculate the polarization purity, $\eta = \Phi_z / (\Phi_z + \Phi_r)$, $\Phi_{r,z} = 2\pi \int_0^\infty |E_{r,z}(r,z)|^2 \, r dr$, defined as the percentage of the longitudinally polarized electric energy to the total electric energy [12]. The needle purity is calculated to be $\eta = 99.9\%$ in the focal plane ($z = 0$), and $\eta > 98.5\%$ throughout the entire DOF region, for all of lengths L. This means that the created optical needle is nearly entirely polarized longitudinally along the entire DOF extent. The purity is higher than that reported in [23, 25]. The required incident field $\vec{E}_i(r)$ in the normalized pupil plane for generating such optical needle can be computed by Eq. (3). For $L = N\lambda$ ($N = 1, 2, 3...$), the input field is radially polarized with N annular bright belts separated by dark rings, and the maximum of bright belts increases monotonically from the innermost to the outermost belt (see Fig. 2(d)).

3.2 Generation of double-focus with prescribed spacing

For another example, the calculated pupil illumination pattern shown in Fig. 2(d) can also be used to generate a double-focus with prescribed separation. This is realized by choosing the illumination pattern $\vec{E}_i(r)$ at the pupil plane of the left objective and right objective (refer to Fig. 1) to be the same instead of having opposite phase. The results are illustrated in Fig. 3. The spacing between two spots $\sim L$ depends on the length of uniform line source. The FWHM of all spots plotted in Fig. 3 are computed to be 0.36λ in the transversal direction and to be $\sim \lambda$ in the axial direction.

The phenomena that the focusing of radiation pattern from the uniform line source exhibits the optical needle or the double-focus with prescribed characteristics can be interpreted by the interference of two counter-propagating incident beams [17]. Constructive interference within the entire DOF occurs when the phase between two counter-propagating beams has a relative π-phase shift. This occurrence generates the on-axis optical needle. However, when the two counter-propagating incident beams have no phase difference, the intensity within the entire DOF becomes dark owing to the destructive interference. But the phases at the two ends of the uniform line source exhibit an abrupt π-phase jump (see Fig. 2(b)), leading to the creation of a double-focus pattern separated by the length of the uniform line source.

It is found from calculations that both the DOF of the optical needle and the interval between double-focus are determined by and proportional to the length of uniform line source when $L \geq \lambda$, as illustrated in Fig. 4. However, it is worth pointing out that when $L < \lambda$ or $L \to 0$, the distances, i.e, DOF and interval, remain almost unchanged (see Fig. 4), due to the diffraction limit.

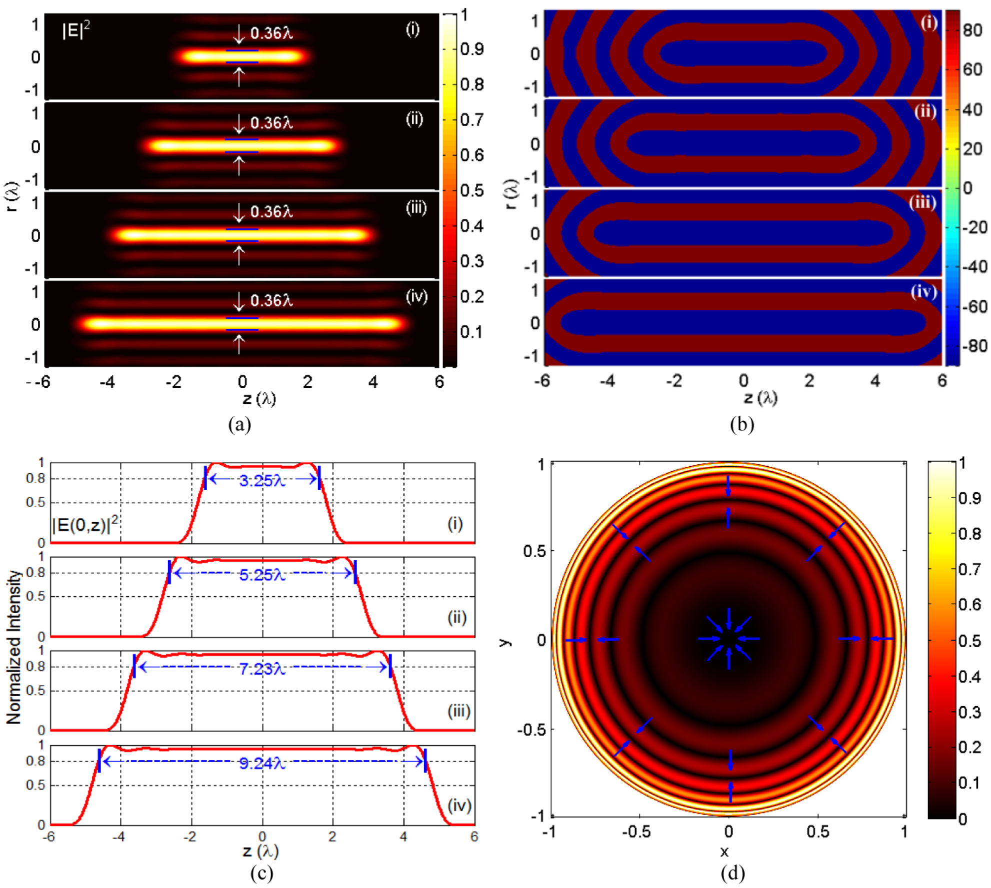

Fig. 2. Generation of optical needle with different lengths by illuminating the 4Pi focusing system with two counter-propagating radially polarized beams $\vec{E}_i(r)$ with a relative π phase shift. (a) total electric energy densities $|E|^2$ in the r-z plane, (b) corresponding phase distributions of the E_z component, and (c) axial electric energy densities $|E(0,z)|^2$ for (i) $4\lambda-$, (ii) $6\lambda-$, (iii) $8\lambda-$, (iv) $10\lambda-$ length uniform line source, respectively; (d) input field distribution at the normalized pupil plane for $L = 8\lambda$.

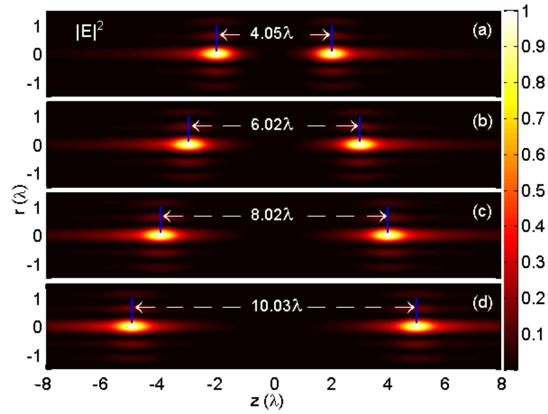

Fig. 3. Generation of double-focus with alterable interval by illuminating the 4Pi focusing system with two counter-propagating radially polarized beams $\vec{E}_i(r)$ with same-phase. Total electric energy densities $|E|^2$ in the r-z plane for (i) $4\lambda-$, (ii) $6\lambda-$, (iii) $8\lambda-$, (iv) $10\lambda-$ length uniform line source, respectively.

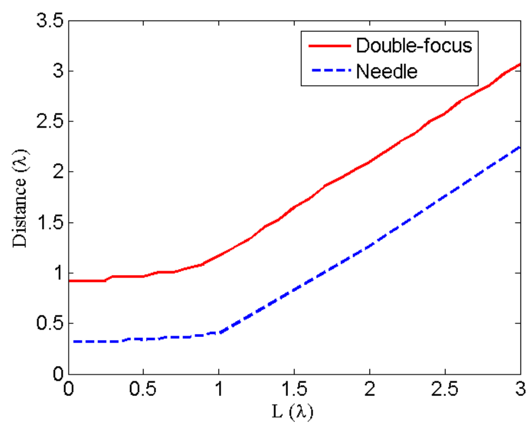

Fig. 4. DOF of optical needle and spacing between double-focus versus length of uniform line source.

4. Conclusions

In conclusions, we have presented a simple and flexible method to engineer optical focal field with prescribed characteristics by reversing the field pattern radiated from a uniform line source situated at the focus of a 4Pi focusing system formed by two confocal high-NA objective lenses. Arbitrarily long optical needle and coaxial double-focus with desired spacing are illustrated as examples. It is demonstrated that optical needle field with transversal spot size of $\sim 0.36\lambda$ (FWHM), high longitudinal polarization purity ($\eta > 98.5\%$) throughout the entire DOF region, and high uniformity of axial energy density can be easily created by illuminating the 4Pi focusing system with two counter-propagating radially polarized beams $\vec{E}_i(r)$ with π phase difference. If the phase different of input field $\vec{E}_i(r)$ is chosen to be 0 instead, double-focus with beam size of 0.36λ in transversal direction and $\sim \lambda$ in axial direction can be obtained. The DOF of optical needle and the spacing of double-spot depend on the length of uniform line source. The required illumination at the pupil plane for creating desired focusing pattern can be found through solving the radiation field of uniform line source located at the focus of 4Pi focusing system. Compared with previously reported

#232538 - $15.00 USD Received 15 Jan 2015; revised 2 Mar 2015; accepted 4 Mar 2015; published 13 Mar 2015

methods, this new method does not require any optimization, which significantly simplifies the design procedure. The realization of complex illumination pattern at the pupil is attainable nowadays by using the latest technologies of spatial light modulation and nanofabrication [32]. These special focusing patterns might found their applications in particle acceleration, optical microscopy, optical trapping and manipulations.

Acknowledgments

This work is supported by the Key Project of Science and Technology Department of Fujian Province (No. 2012H0035), the Key Lab of Information Functional Materials for Fujian Higher Education, and the Key Discipline of Electronic Science and Technology.